Global disruption of the cerebellar transcriptome in a Down syndrome mouse model

Nidhi G. Saran[1], Mathew T. Pletcher[1,†], JoAnne E. Natale[2], Ying Cheng[2] and Roger H. Reeves[1,*]

[1]Department of Physiology, Johns Hopkins School of Medicine, Baltimore, MD 21210, USA and [2]Research Centers for Genetic Medicine and Neuroscience, Children's National Medical Center, 111 Michigan Avenue, NW, Washington, DC 20010, USA

Trisomy 21 (Down syndrome) results in cerebellar dysmorphology with direct parallels in the Ts65Dn mouse. Despite pronounced changes in morphology, cerebellar function is not markedly different. As a first test of whether those cerebellar cells that have survived to adulthood in trisomic mice are equivalent to euploid cells, we used microarrays to assess the trisomic and euploid cerebella. Trisomic and euploid transcriptomes were robustly distinguished. Changes in expression of individual genes were very subtle, but the differences in respective transcriptome phenotypes extended deeply into the set of nearly 7000 probes (genes) located throughout the genome. In contrast to deterministic models of gene action in trisomy, examination of the discriminating genes in two independent experiments suggests that the global perturbation includes a significant stochastic component. Thus, dosage imbalance of 124 genes in Ts65Dn mice alters the expression of thousands of genes to create a variable trisomic transcriptome. This global destabilization has important implications for approaches to ameliorative therapies in Down syndrome.

INTRODUCTION

Trisomy for human chromosome 21 (HSA21) causes Down syndrome (DS), the most common live-born human aneuploidy. The central nervous system is invariably affected in DS, resulting in structural changes, mental retardation and appearance of Alzheimer disease-like neurohistopathology by the fourth decade. More than 80 clinical features may occur in DS, including facial and skeletal features, congenital defects of the gut and heart, male infertility and an increased incidence of leukemia (1). The majority of these DS features are not present in every individual and the features that are present often vary significantly in terms of severity. Little is known about the mechanisms by which dosage imbalance for normal HSA21 genes results in the various clinical aspects of the syndrome.

The distal end of mouse chromosome 16 (MMU16) shows near-perfect conserved synteny with HSA21 (2,3). The Ts65Dn mouse has segmental trisomy for a substantial part of this region which includes orthologs of 124 of the 238 known and predicted HSA21 genes (4). It shows decreased nociception (5); hyperactivity (6,7); and displays deficits in spatial learning

and in working and long-term memory that are analogous to those in DS (6–8).

The Ts65Dn mouse and humans with DS also have similar alterations in brain morphology. Quantitative cellular changes in regions of the hippocampus (9) and a reduction of asymmetric synapses in the temporal cortex (10) have been reported in Ts65Dn mice. In humans with DS, the volume of the brain is reduced and the cerebellum is reduced to an even greater extent (11). An analogous cerebellar phenotype has been established in the Ts65Dn murine model of DS. Assessment of Ts65Dn cerebella identified a significant reduction in cerebellar granule cell density which was also shown to occur in individuals with DS (12).

Despite alterations in morphology and granule cell density in Ts65Dn mice, the animals do not display a deficit in standard rotarod paradigms (13). This raises questions about how trisomy affects cerebellar neurons. The granule cells that survive to adulthood may be essentially normal, functional cells, but with abnormal numbers and connections due to perturbations of cerebellar development caused by trisomy. Alternatively, the dosage imbalance of a small fraction of genes could be amplified to produce large downstream

Table 1. Elevated transcript levels for genes at dosage imbalance

HSA3 and HSA22 orthologs on MMU16						HSA21 orthologs on MMU16		
GenBank	Gene Name	Ts/Eu ratio	GenBank	Gene Name	Ts/Eu ratio	GenBank	Gene Name	Ts/Eu ratio
HSA3; Average Ts/Eu ratio: 0.93			X57349	*Trfr*	1.03	HSA21; Average Ts/Eu ratio: 1.45		
L25274	*Alcam*	0.72	D16464	*Hes1*	1.03	X66118	*Grik1*	0.84
X51468	*Sst*	0.75	AB031291	*Tagln3*	1.07	Y09864	*Ifnar2* (partial)	1.08
U84207	*Pcyt1a*	0.76	U41465	*Bcl6*	1.08	AJ239082	*Sh3bgr*	1.17
M91380	*Fstl*	0.80	AB010152	*Trp63*	1.09	AI047617	Unknown	1.17
AF037260	*Tnk2*	0.80	L13290	*Adprh*	1.09	AB008516	*Ttc3*	1.19
X57349	*Trfr*	0.80	U20619	*Kpna1*	1.10	U20892	*Gart*	1.26
U13837	*Atp6v1a1*	0.81	X12507	*Eif4a2*	1.12	J04103	*Ets2*	1.27
AB019003	*Abcc5*	0.82				J03368	*Mx2*	1.28
D16333	*Cpo*	0.85				U58497	*Dyrk1a*	1.30
AF029215	*Mox2*	0.85	HSA22; Average Ts/Eu ratio: 1.08			M35725	*Sod1*	1.40
X82648	*Apod*	0.85	U82758	*Cldn5*	0.79	M89641	*Ifnar1*	1.44
X66976	*Col8a1*	0.91	U64445	*Ufd1l*	0.92	AB001990	*Dscr3*	1.44
U66201	*Fgf12*	0.91	AJ130961	*Ube2l3*	0.95	U53696	*Il10rb*	1.45
X80232	*Silg41*	0.91	X56045	*Ranbp1*	0.97	U69599	*Ifngr2*	1.49
U13837	*Atp6v1a1*	0.92	X95480	*Dgcr2*	0.97	Z37164	*Cct8*	1.53
L27439	*Pros1*	0.93	AB013603	*Top3b*	1.00	X53476	*Hmgn1*	1.59
D16333	*Cpo*	0.95	AB027566	*Txnrd2*	1.03	D67076	*Adamts1*	1.62
AB012693	*Cd47*	0.98	U07425	*Serpind1*	1.04	X17320	*Pcp4*	1.63
AF022110	*Itgb5*	0.99	AF021031	*Dgcr6*	1.06	U31966	*Cbr1*	1.64
AF032995	*Crygs*	0.99	AF076156	*Comt*	1.11	U05245	*Tiam1*	1.66
U93309	*Dlgh1*	0.99	AF034092	*Mrpl40*	1.15	AF013486	*Ifnar2*	2.93
U80078	*Zfp148*	1.01	AF033350	*Sept5*	1.17			
U27106	*Ap2m1*	1.02	D87271	*Mapk1*	1.35			
			AB001419	*Gp1bb*	1.67			

Transcript ratios for all 45 annotated MMU16 genes on the arrays, corresponding to HSA3, HSA21 and HSA22 orthologs. The average Ts/Eu ratio of the HSA21 orthologs on MMU16 was 1.45. The over expression of the HSA21 orthologs at dosage imbalance in the Ts65Dn mouse is statistically significant; P-value for a Student's t-test between orthologs of HSA3 and HSA21 is 9.4×10^{-6}; HSA22 and HSA21 is 1.5×10^{-3}.

effects, perturbing the transcriptome of every cell. These scenarios have very different implications for therapeutic approaches to ameliorate the effects of trisomy.

Characterization of the transcriptomes of euploid (Eu) and trisomic (Ts) cerebella represents an essential step towards understanding the effect and mechanism of action of dosage imbalance in brain development. Mao *et al.* (14) used microarray analysis to demonstrate an overall up-regulation of HSA21 transcripts in frozen human fetal brain samples and astrocyte cell lines derived from fetal brain. Serial analysis of gene expression was also used to study the transcriptome of the whole Ts65Dn and Eu adult brain (15). Only 330 of 45 000 TAGs were present in sufficient numbers to show a significant difference between Ts and Eu brain. Of the 124 HSA21 orthologs at dosage imbalance in Ts65Dn mice, which are expected to be present at about 1.5-fold of Eu levels on average, 15 were detected but only three occurred with sufficient frequency to suggest that they were differentially expressed.

In this study, we created expression profiles of the Ts65Dn and Eu adult cerebella using a sensitive microarray platform to examine more than 12 000 genes. The cerebellar gene expression profiles provided a robust phenotype that discriminated between Ts and Eu mice. Trisomy produced a global destabilization of the transcriptome in Ts animals, substantially altering levels of more than one-third of the expressed genes and suggesting that there is an intrinsic, global disruption of transcript levels in cells of the trisomic cerebellum.

RESULTS

Microarrays detect elevated expression of HSA21 orthologs

We used Affymetrix microarrays to examine the expression profiles of 12 488 probes in the Ts65Dn and Eu cerebellum of 3–4-month-old, adult male mice in two independent experiments. Each of 18 RNA samples was hybridized to duplicate chips. Any chips or samples with parameters falling outside of stringent quality control standards were removed, resulting in 13 samples (26 chips) for analysis. Of the 12 488 probes on the U74Av2 chip, we further eliminated probes that were absent from 20 or more of the 26 chips, evenly distributed between Ts and Eu, based on the perfect match/mismatch algorithm of Affymetrix. The resulting set included 6902 probes.

The U74Av2 chip includes 204 MMU16 probes of which 23 are reported to be HSA21 orthologs; 21 of those are at dosage imbalance in the Ts65Dn mouse. The average Ts : Eu expression ratio was significantly higher for triplicated HSA21 orthologs than for other MMU16 genes (Table 1). In experiment 1 the average ratio of Ts : Eu expression for HSA21 orthologs was 1.45 (range 0.84–2.93) whereas the average ratio for the disomic genes on MMU16 was 1.01 ($P = 8.05 \times 10^{-5}$; Student's t-test). The Ts65Dn chromosome could also be discriminated from all other chromosomes by expression ratios of probes based on the chromosome of origin (Supplementary Material Fig. 1). Thus, the platform had sufficient sensitivity to detect the expected transcript level changes between Eu and Ts that result directly from dosage imbalance.
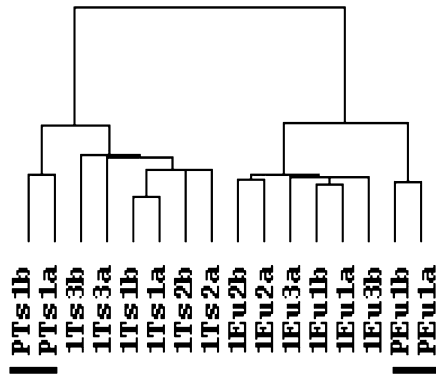
Figure 1. Cluster analysis discriminated between Ts and Eu transcriptomes. Three pairs of Ts and Eu samples and one pair of pooled samples (three individuals per pool) were segregated based on genotype. Pooled samples tend to normalize individual variation and were separated from individuals within each group. Therefore, individual values were considered separately for analysis.

Robust differences in trisomic and euploid transcriptomes

RNAs were analyzed from three individuals and one pool of Eu, and matched RNAs from Ts mice in experiment 1. Hierarchical data clustering across genes and arrays was performed using the program Cluster (16). Cluster analysis effectively discriminated between Ts and Eu pools, but not surprisingly, separated the pooled samples from the individuals (Fig. 1). Therefore, we chose to exclude the pooled samples, leaving the results from the three pairs of Ts and Eu mice (12 Affymetrix chips) for subsequent analyses. Hierarchical trees were then generated from the individual RNA results. This analysis clearly discriminated between Ts and Eu mice, grouping them in two separate clusters (Fig. 2A). We used several methods to characterize the distinct transcription pattern in Ts cerebella (Fig. 2 and Supplementary Material Fig. 2).

First, the ratio values for each gene-hybridization were used to select probes that were most consistently different between the Ts and Eu data sets. We selected a discrete group of 1532 'highly discriminating probes' that were upregulated in all six Ts and downregulated in all six Eu, up in five Ts and down in six Eu, and up in six Ts and down in five Eu, or vice versa. Hierarchical clustering performed on these highly discriminating probes alone distinguished between Ts and Eu (data not shown). Moreover, removing these 1532 highly discriminating probes, 22% of the 6902 hybridizing probes, did not abolish clustering of Ts separately from Eu (Fig. 2B). That is, the remaining 5370 probes completely discriminated between Ts and Eu cerebella. Further, removal of an additional 1039 'moderately discriminating probes' that were upregulated in five Ts and downregulated in five Eu, up in six Ts and down in four Eu, and up in four Ts and down in six Eu, or vice versa, were removed (37% of the total probe set), did not abolish the perfect separation between Ts and Eu transcriptomes (Fig. 2C). The ability to discriminate between Ts and Eu cerebellar transcriptomes was lost only after we eliminated 3652 (53%) of the probes that were most consistently different between Ts and Eu (Fig. 2D).
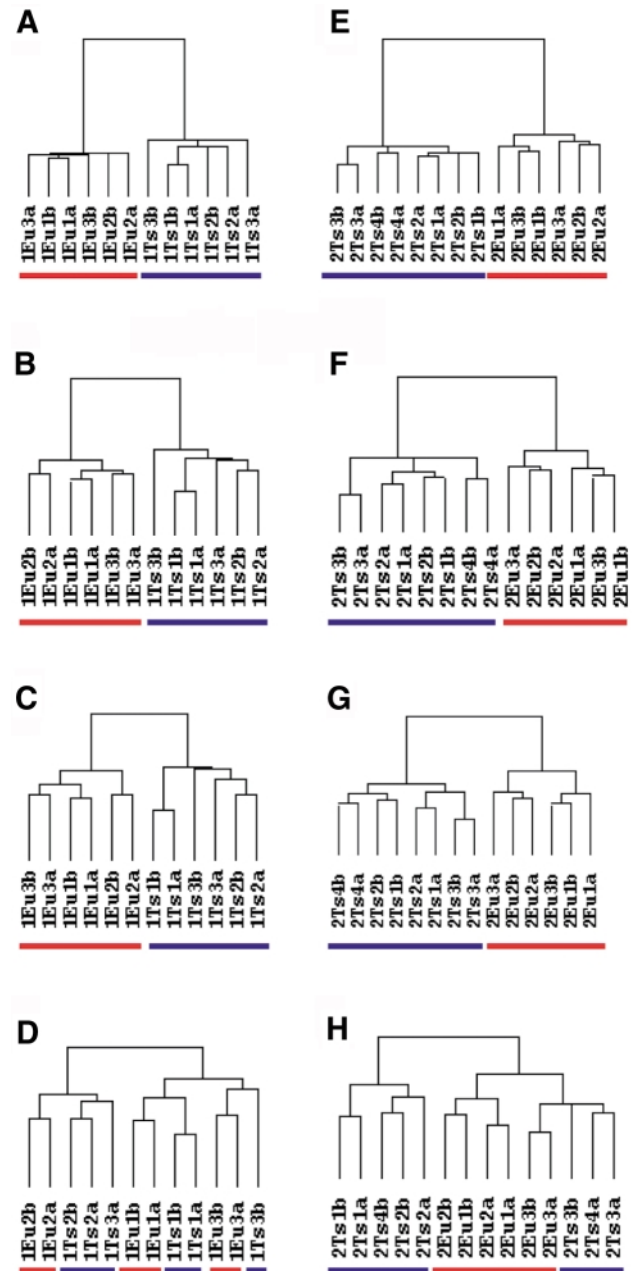

Figure 2. Thousands of genes were differentially expressed in Ts versus Eu mice. Normalized data were clustered across genes and arrays. Trees generated for experiments 1 (**A**) and 2 (**E**) clearly distinguish the Ts and Eu samples into two distinct groups. Cluster analysis performed after eliminating discriminators showed that even upon eliminating more than one-third of the data set, consisting of the most discriminating genes, Eu and Ts samples were clustered separately from each other. (A–D), Experiment 1; (**B**), 1532 of the most consistently different ('highly discriminating') probes were eliminated; (**C**) 2571 of the most discriminating probes were removed; (**D**) clustering broke down only upon removal of 3652 differentially expressed genes. (E–H) Experiment 2; (**F**) 1675 highly discriminating probes were eliminated; (**G**) 2414 of the most discriminating probes were removed; (**H**) clustering was disturbed only after removing 2875 probes.

In a second approach to characterize the extent of differences between the Ts and Eu cerebellar transcriptomes, we removed the genes that showed the greatest fold difference in expression. Twenty-two percent, or 1078 probes, had a Ts : Eu expression
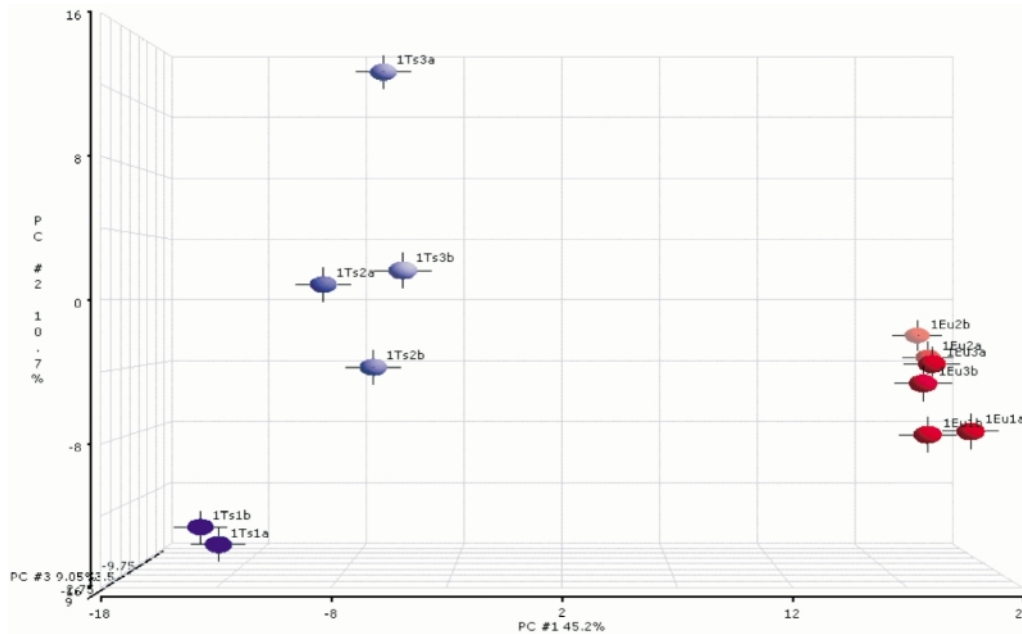
Figure 3. Ts transcriptomes were more variable than Eu. PCA was performed on normalized gene expression levels for each Ts and Eu sample in experiment 1. The first three principal components accounted for 64.9% of data variance. PCA clearly discriminated between the two genotypes.

ratio >1.2 or <0.8. The remaining 5824 genes, which changed 20% or less, readily distinguished Ts and Eu. The groups were readily distinguished even when the fold change was dropped to 16%, eliminating 1610 probes with the biggest Ts : Eu difference from the analysis.

Next, we identified genes with significantly different signal intensity between Ts and Eu samples. A total of 277 probes showed a significant difference in expression at a level of $P < 0.01$, with 922 at a level of $P < 0.05$. Ts and Eu cerebellar transcriptomes were readily distinguished after removal of these 922 probes. Finally, the SNOMAD program (17) was used to identify probes that were most different between the two samples based on Z-score. Only 26 probes had a score of $Z > 3$; at $Z > 2$, 136 probes were identified. Their removal did not affect the ability to discriminate Ts and Eu cerebellar transcriptomes (Supplementary Material Fig. 2).

This deep alteration in the cerebellar transcriptome, in which thousands of genes were expressed differently as a result of trisomy, was verified in an independent experiment using paired chips hybridized with RNA from three Eu and four Ts mice. Eu versus Ts clustering was maintained upon removal of 1675 highly discriminating probes (24%) and persisted after the removal of 2414 most discriminating probes (35%). The discrimination between Ts and Eu broke down only upon elimination of 2875 probes, 42% of the total (Fig. 2E–H). Analysis of experiment 2 using the same additional criteria for probe selection as in experiment 1 produced the same results: removal of a large proportion of genes whose expression was most different in Ts and Eu did not eliminate the ability to discriminate between them. Thus, dosage imbalance for a few genes disrupted the steady state levels of thousands of transcripts in the cerebellum.

Stochastic effects of transcripts in trisomic mice

Prevailing notions of gene action in DS are deterministic; that is, the defined dosage imbalances are believed to initiate specific downstream gene expression cascades, resulting ultimately in characteristic DS phenotypes. In contrast to this expectation, comparison of the sets of ~2500 discriminating probes identified in experiments 1 and 2 (Fig. 2C and G) showed that only 939 (~38%) were present in both sets (Supplementary Material Table 1). Fourteen of the 21 HSA21 orthologs at dosage imbalance in the Ts65Dn mice were found in this set of common probes. To characterize these common genes, we annotated the probe set by functional keyword and chromosomal position in the mouse genome. Based on the keyword annotation, available for 26% of all probes, no single functional group was found to dominate the discriminating genes in either experiment. Chromosomal position is available for 96% of the probes. Clustering the probes based on their chromosome of origin successfully discriminated between Ts and Eu for all chromosomes (Supplementary Material Fig. 3), that is genes that are dysregulated by trisomy occur throughout the genome. However, as with functional categories, no one chromosome was found to dominate the region of discriminating genes. These genes were distributed evenly over all murine chromosomes. Comparison of differentially expressed probes selected by other criteria gave similar results.

Variability of trisomic transcriptomes

We performed principal components analysis (PCA) on the data from experiment 1 as another measure of similarity or difference between the Ts and Eu RNA sets (Fig. 3). In the PCA plot, the first principal component axis clearly separated

Ts and Eu transcriptomes, and accounted for 45.2% of the variance in the data set. We observed substantially greater variability among the expression profiles of Ts samples compared to Eu.

DISCUSSION

We have shown, in replicate array experiments, that hierarchical data clustering of transcriptome profiles separated Ts from Eu mice, that is steady state adult cerebellar gene expression levels robustly discriminated between the two groups. The average change in transcript level per gene was small; only 1078 of 6902 probes varied by more than 20% and only 29 were misexpressed 2-fold or more (Table 2). Of these 29, only six varied to the same degree in the replicate experiment. This is consistent with the observations of Mao *et al.* (14) who examined gene expression of triplicated (HSA21) genes in DS human fetal brain and cultured astrocytes. They found that while *collective* changes in expression of all HSA21 genes were upregulated in trisomic samples, no *individual* gene was significantly altered.

While the magnitude of transcript level change in individual genes was small, the number of genes affected was substantial. More than a third of the genes whose expression was most consistently different between Ts and Eu could be removed from the clustering and the samples were still parsed correctly. Thus dosage imbalance produces a global alteration of the cerebellar transcriptome.

We found no evidence that the discriminating probes were physically grouped in the mouse genome and no substantial differences between the Ts and Eu samples in genes from specific functional classes, including transcription factors, signaling molecules, apoptosis, cell cycle, DNA synthesis, growth factors and receptors, neurotransmitters, and cytoskeleton. Kadota *et al.* (18) reported elevated levels of apoptosis in neuronal stem cells differentiated from mouse ES cells containing a human Chr21, and Wolvetang *et al.* (19) recently reported that over expression of *Ets2* in transgenic mice and murine and human cell lines leads to an increase in apoptosis via activity in the *p53* pathway. Seven apoptosis- and five *p53*-related probes were queried in the Affymetrix data set and none was misexpressed in the Ts samples. However, less than a third of the probes on the U74Av2 chip can be classified into functional categories. A more thorough classification might detect a subtle pattern of misexpression within a functional class of genes.

PCA showed an important trend in that Eu transcriptomes were clustered much more tightly than those of Ts cerebella (Fig. 3). This variation was reflected qualitatively in the discriminating probe sets that differentiated Ts and Eu cerebellar transcriptomes. While the number of consistently discriminating probes was similar in two independent experiments (Fig. 2C and G), only 38% of these 2500 probes were common to both experiments. DS is characterized by a broad range of anomalies, subsets of which are present in a given individual with trisomy 21 and only a few of which are always present. Those features that are present display a variable pattern of expressivity among individuals. Our results correlate qualitative differences that make up the global transcript level

Table 2. Probes showing 2-fold or greater change in expression

GenBank	Gene Name	Ts/Eu (Expt 1)	Ts/Eu (Expt 2)
U73478	*Anp32a*	0.26	0.81
AI507266	Unknown	0.30	1.41
AV212851	Unknown	0.36	0.76
AV239611	Unknown	0.41	0.94
AA986395	Unknown	0.42	0.95
AI852838	Unknown	0.42	1.22
Y13832	*Meg3*	0.43	1.15
AV068234	Unknown	0.44	0.09
AF038939	*Peg3*	0.45	0.88
AV319920	Unknown	0.45	0.69
AF071068	*Ddc*	0.46	0.84
Y00208	*Hoxa5*	0.47	0.54
AI561567	Unknown	0.50	1.00
AV157222	Unknown	2.00	0.81
Y11666	*Hk2*	2.03	0.77
U29056	*Sla*	2.09	1.32
AJ007909	*Edr*	2.11	1.17
AF109906	Unknown	2.13	1.3
AA815795	Unknown	2.16	1.93
AI842217	Unknown	2.25	1.06
AW124933	Unknown	2.25	1.50
AA617494	Unknown	2.37	0.61
AA710297	Unknown	2.50	0.96
M83218	*S100a8*	2.73	0.46
X81584	*Igfbp6*	2.80	1.11
M83219	*S100a9*	2.84	0.37
AF013486	*Ifnar2*	2.93	2.75
AJ006584	*Eif2s3y*	4.14	0.88
AB014485	*Scap2*	5.65	1.07

Only 29 probes showed a 2-fold or greater change between Ts and Eu samples in experiment 1. Expression ratios for experiment 2 are shown for comparison. *Ifnar2* is the only gene among these that is at dosage imbalance in Ts65Dn mice. The expression levels of all other probes in experiment 1 changed less than 2-fold.

variations with phenotypic variability. Further more, the substantial difference in affected genes suggests that stochastic effects are important in shaping the trisomic transcriptome.

We showed previously that granule cells are reduced in density (to 80% of Eu) in Ts65Dn mice (and in DS) while Purkinje cells are decreased about 10% (12). Granule cells represent >90% of all cells (and 95% of neurons) in the adult cerebellum (20) and thus their RNA comprises most of the signal in the array experiments. We therefore considered the possibility that the changes in expression profiles between Ts and Eu resulted from an altered cellular composition of the cerebellum. If neuronal populations were disproportionately depleted, the expression ratio of astrocyte- to neuron-specific markers should increase. However, no difference was detected in the expression level of the astrocyte-specific marker, glial fibrillary acidic protein (GFAP) in the Ts and Eu samples, and no change occurred in the ratio of GFAP to neurofilament-H or -M expression, suggesting that the relative signal contribution from astrocytes and neurons remained the same. The same result was seen with vimentin, a second astrocyte marker represented in the U74Av2 probe set. In addition, we looked at the expression of 62 probes identified as belonging to the categories of neurogenesis, neuropeptide, neurone, and neurotransmitter and synapse. The average Ts : Eu ratio of these probes was 0.94. Extensive quantitative morphological analysis

of the Ts and Eu cerebellum, quantitation of the relative contributions of mRNA from different cell populations, and the possibility that morphologically identical granule cells actually represent distinct classes of neurons affected differently by trisomy will have to be examined to establish absolutely whether shifts in relative sizes of neuronal and astrocyte populations are responsible for the array results presented here. In these experiments, we did not find evidence for a change in cell populations that would account for the global transcriptome changes.

If cell populations are not disproportionately altered, then our results are best explained by a substantial cell autonomous alteration of the transcriptome. The transcript level changes of individual genes that differentiate Ts and Eu cerebella are subtle, but collectively, a small increase in transcript levels of 124 genes at dosage imbalance results in altered steady state levels for thousands of mRNAs. Further more, a substantial portion of the altered transcripts may arise from stochastic, not deterministic consequences of dosage imbalance.

Whether trisomy causes developmental perturbations that shift cell populations or disrupts the transcriptome of every cell, or both, it may be difficult to reverse these situations in adults. Analysis of gene expression profiles in the cerebellum at the critical developmental stages at which the cells are generated and differentiate will help to identify the most likely targets and times for ameliorative interventions.

MATERIALS AND METHODS

RNA

Ts65Dn mice were obtained from the Jackson Laboratory as an advanced intercross of C57BL/6JEi and C3H/HeSnJEi. Age-matched, 3–4-month-old, male Ts65Dn and control mice were produced at Johns Hopkins School of Medicine or at the Eleanor Roosevelt Cancer Institute. Mice were euthanized and brains were removed and rapidly dissected. All procedures were approved by the Institutional Animal Care and Use Committee. Cerebella were homogenized by aspiration with a sterile 10G syringe in Trizol (Invitrogen, CA). Total RNA was isolated from each cerebellar sample according to the manufacturer's instructions and further purified using an RNeasy kit (Qiagen, Valencia, CA) prior to quantification. Purified RNA was examined on agarose gels to eliminate degraded samples.

cRNA probe preparation and hybridization

Procedures for cRNA preparation and GeneChip processing were performed as previously described (21,22). Briefly, two $7\,\mu g$ aliquots of total RNA from each tissue sample, processed in parallel, were converted into double stranded cDNA with an oligo-dT primer containing T7 RNA polymerase promoter. Purified double stranded cDNA was converted to biotin-labeled cRNA (ENZO Diagnostics, NY). Each fragmented cRNA sample was hybridized to mouse U74Av2 oligonucleotide microarray (Affymetrix, Santa Clara, CA) for 16 h at 60 rpm at 45°C. The mouse U74Av2 microarray contains 12 488 full-length sequences and expressed sequence tags (referred to as probe sets or genes throughout this text). After hybridization,

each microarray was then washed and stained on the Affymetrix Fluidics Station 400 using instructions and reagents provided by Affymetrix. Raw intensity data were captured and the Affymetrix GeneChip® software MAS 5.0 was used to calculate signal intensity values for each oligonucleotide probe set. A scaling factor, with a target intensity of microarray sector fluorescence to 800, was automatically applied to each microarray by the MAS 5.0 algorithm, permitting reproducible inter-array comparisons. Probe sets hybridization performance (pairs of 20 perfect match and mismatch 25mer oligonucleotides per probe sets) identified signal intensities that were reliably detected as present, and eliminated most non-specific cross-hybridization signals, as previously described (21,22). The range of values and acceptable limits (in parentheses) for experiments 1 and 2 were 0.56–1.12 and 0.29–0.42 for scaling factor (<4), 48.3–52.1% and 47.4–53.5% (43–55%) for proportion of present probe sets, $R = 0.96$–0.99 and $R = 0.93$–0.99 for observed correlation between signal values for each gene between microarrays obtained from the same RNA.

Signal processing

Within both species, each microarray underwent a stringent quality control evaluation as previously described (22). We used the Agilent G2500A Gene Array Scanner, with a high setting for the photomultiplier tube to maximize sensitivity of low abundant transcripts at the expense of intensity saturation of high abundant transcripts. Therefore, we used an algorithm to detect probe sets that became saturated by the biotin/streptavidin/phycoerythrin amplification (T. Teslovich, manuscript in preparation). For each of these probe sets, the saturated intensity value was replaced with non-saturated intensity signal generated by the initial streptavidin/phycoerythrin scan across all microarrays in the experiment.

Gene expression data analysis

In each experiment, the average Ts : Eu ratio for each probe was generated by dividing the average Ts signal across all microarrays by the average Eu signal across all microarrays, for that probe. Gene expression data were initially normalized by dividing the signal intensity of each probe by the average signal intensity of that probe in all samples. This resulted in trees that separated Ts and Eu into two clusters. However, the differentially expressed genes were not easily identifiable. In order to amplify the visual differences, we generated normalized ratios by dividing the signal intensity of each Ts sample by the average Eu signal and the signal intensity of each Eu sample by the average Ts signal. We confirmed that this manipulation resulted in the same clustering patterns as before and the trees were more successful in visually displaying the differentially expressed probes.

The normalized data set was used for Cluster analysis and PCA. Cluster analysis was performed using the program Cluster and the trees were viewed with Treeview (16). PCA was performed with the Partek Pro software (Partek, MI). Data set annotation was performed using the 'annotate' tool of the Database Reference of Array Genes Online (DRAGON) (23) website (http://pevsnerlab.kennedykrieger.org/dragon.htm) in conjunction with the blast tools on the Affymetrix website

(www.affymetrix.com). Affymetrix probe sequences were also BLAT mapped against the Celera Mouse assembly R13 (24).

SUPPLEMENTARY MATERIAL

Supplementary Material is available at HMG Online and http://inertia.bs.jhmi.edu.

ACKNOWLEDGEMENTS

REFERENCES

1. Epstein, C.J., Korenberg, J.R., Anneren, G., Antonarakis, S.E., Ayme, S., Courchesne, E., Epstein, L.B., Fowler, A., Groner, Y., Huret, J.L. *et al.* (1991) Protocols to establish genotype-phenotype correlations in Down syndrome. *Am. J. Hum. Genet.*, **49**, 207–235.
2. Mural, R.J., Adams, M.D., Myers, E.W., Smith, H.O., Miklos, G.L., Wides, R., Halpern, A., Li, P.W., Sutton, G.G., Nadeau, J. *et al.* (2002) A comparison of whole-genome shotgun-derived mouse chromosome 16 and the human genome. *Science*, **296**, 1661–1671.
3. Pletcher, M.T., Wiltshire, T., Cabin, D.E., Villanueva, M. and Reeves, R.H. (2001) Use of comparative physical and sequence mapping to annotate mouse chromosome 16 and human chromosome 21. *Genomics*, **74**, 45–54.
4. Gitton, Y., Dahmane, N., Baik, S., Ruiz i Altaba, A., Neidhardt, L., Scholze, M., Herrmann, B.G., Kahlem, P., Benkahla, A., Schrinner, S. *et al.* (2002) A gene expression map of human chromosome 21 orthologues in the mouse. *Nature*, **420**, 586–590.
5. Martinez-Cue, C., Baamonde, C., Lumbreras, M.A., Vallina, I.F., Dierssen, M. and Florez, J. (1999) A murine model for Down syndrome shows reduced responsiveness to pain. *Neuroreport*, **10**, 1119–1122.
6. Escorihuela, R.M., Fernandez-Teruel, A., Vallina, I.F., Baamonde, C., Lumbreras, M.A., Dierssen, M., Tobena, A. and Florez, J. (1995) A behavioral assessment of Ts65Dn mice: a putative Down syndrome model. *Neurosci. Lett.*, **199**, 143–146.
7. Reeves, R.H., Irving, N.G., Moran, T.H., Wohn, A., Kitt, C., Sisodia, S.S., Schmidt, C., Bronson, R.T. and Davisson, M.T. (1995) A mouse model for Down syndrome exhibits learning and behaviour deficits. *Nat. Genet.*, **11**, 177–184.
8. Demas, G.E., Nelson, R.J., Krueger, B.K. and Yarowsky, P.J. (1998) Impaired spatial working and reference memory in segmental trisomy (Ts65Dn) mice. *Behav. Brain Res.*, **90**, 199–201.
9. Insausti, A.M., Megias, M., Crespo, D., Cruz-Orive, L.M., Dierssen, M., Vallina, I.F., Insausti, R., Florez, J. and Vallina, T.F. (1998) Hippocampal volume and neuronal number in Ts65Dn mice: a murine model of Down syndrome. *Neurosci. Lett.*, **253**, 175–178.
10. Kurt, M.A., Davies, D.C., Kidd, M., Dierssen, M. and Florez, J. (2000) Synaptic deficit in the temporal cortex of partial trisomy 16 (Ts65Dn) mice. *Brain Res.*, **858**, 191–197.
11. Raz, N., Torres, I.J., Briggs, S.D., Spencer, W.D., Thornton, A.E., Loken, W.J., Gunning, F.M., McQuain, J.D., Driesen, N.R. and Acker, J.D. (1995) Selective neuroanatomic abnormalities in Down's syndrome and their cognitive correlates: evidence from MRI morphometry. *Neurology*, **45**, 356–366.
12. Baxter, L.L., Moran, T.H., Richtsmeier, J.T., Troncoso, J. and Reeves, R.H. (2000) Discovery and genetic localization of Down syndrome cerebellar phenotypes using the Ts65Dn mouse. *Hum. Mol. Genet.*, **9**, 195–202.
13. Hyde, L.A., Crnic, L.S., Pollock, A. and Bickford, P.C. (2001) Motor learning in Ts65Dn mice, a model for Down syndrome. *Dev. Psychobiol.*, **38**, 33–45.
14. Mao, R., Zielke, C.L., Zielke, H.R. and Pevsner, J. (2003) Global up-regulation of chromosome 21 gene expression in the developing Down syndrome brain. *Genomics*, **81**, 457–467.
15. Chrast, R., Scott, H.S., Papasavvas, M.P., Rossier, C., Antonarakis, E.S., Barras, C., Davisson, M.T., Schmidt, C., Estivill, X., Dierssen, M. *et al.* (2000) The mouse brain transcriptome by SAGE: differences in gene expression between P30 brains of the partial trisomy 16 mouse model of Down syndrome (Ts65Dn) and normals. *Genome Res.*, **10**, 2006–2021.
16. Eisen, M.B., Spellman, P.T., Brown, P.O. and Botstein, D. (1998) Cluster analysis and display of genome-wide expression patterns. *Proc. Natl Acad. Sci. USA*, **95**, 14863–14868.
17. Colantuoni, C., Henry, G., Zeger, S. and Pevsner, J. (2002) SNOMAD (Standardization and Normalization of MicroArray Data): web-accessible gene expression data analysis. *Bioinformatics*, **18**, 1540–1541.
18. Kadota, M., Shirayoshi, Y. and Oshimura, M. (2002) Elevated apoptosis in pre-mature neurons differentiated from mouse ES cells containing a single human chromosome 21. *Biochem. Biophys. Res. Commun.*, **299**, 599–605.
19. Wolvetang, E.J., Wilson, T.J., Sanij, E., Busciglio, J., Hatzistavrou, T., Seth, A., Hertzog, P.J. and Kola, I. (2003) ETS2 overexpression in transgenic models and in Down syndrome predisposes to apoptosis via the p53 pathway. *Hum. Mol. Genet.*, **12**, 247–255.
20. Gao, W.O., Heintz, N. and Hatten, M.E. (1991) Cerebellar granule cell neurogenesis is regulated by cell-cell interactions *in vitro. Neuron*, **6**, 705–715.
21. Bakay, M., Chen, Y.W., Borup, R., Zhao, P., Nagaraju, K. and Hoffman, E.P. (2002) Sources of variability and effect of experimental approach on expression profiling data interpretation. *BMC Bioinformatics*, **3**, 4.
22. Chen, Y.W., Zhao, P., Borup, R. and Hoffman, E.P. (2000) Expression profiling in the muscular dystrophies: identification of novel aspects of molecular pathophysiology. *J. Cell Biol.*, **151**, 1321–1336.
23. Bouton, C.M. and Pevsner, J. (2000) DRAGON: Database Referencing of Array Genes Online. *Bioinformatics*, **16**, 1038–1039.
24. Kent, W.J. (2002) BLAT—the BLAST-like alignment tool. *Genome Res.*, **12**, 656–664.